CONSTITUTIVE MODELLING OF ANISOTROPIC TWO-SCALE FLOW

Mohammad Rouhi1[1,2,*], Maciej Wysocki[1,2], Ragnar Larsson[1]

[1] *Department of Applied Mechanics, Chalmers University of Technology, SE-412 96 Gothenburg, Sweden*
[2] *Swerea Sicomp, Box 104, SE-43122 Mölndal, Sweden*
[*] *mohammad.rouhi@chalmers.se*

Keywords: liquid resin infusion, anisotropic permeability, phase compressible continuum, free surface migration,

Abstract:
We recently developed a simulation tool to simulate a quite wide class of infusion processes based on a compressible porous media theory formulation involving three constituents, solid, fluid and pore gas embedded in the voids. The aim of this tool is: firstly to model the highly deformable preform and its interaction with external loading and the intrinsic fluid pressure as well as the resulting changes in permeability, compaction and level of saturation. Secondly, the aim is to track the resin flow front during the infusion process using the continuum formulation itself, thereby avoiding methods like level set, etc. [1]. In this contribution, we present a permeability model applied within the modeling framework to account for anisotropic flow in the fibre bed. The ultimate goal of the approach is to be able to simulate the infusion of high performance, large scale composite structures, in an optimized and controlled fashion.

1 Introduction

Darcy law is commonly used to model the resin flow in composite processing. This model describes the fluid flow in porous media and it typically relates the flow rate Q to the pressure difference over the specimen ($\Delta p/L$) defined as

$$Q = K\frac{A}{\mu}\frac{\Delta p}{L}, \tag{1}$$

where μ is the viscosity and K the permeability. Since both the mechanical and the fluid flow properties (i.e. the permeability) of composites are to a large extent determined by fiber volume fraction, it is common to study the permeability variation with fiber volume fraction, as proposed by Carman [2]. However, in case of unidirectional reinforcement, where the transverse flow is much more constrained as compared to flow along the fibers, isotropic predictions of permeability are false. In this context, a permeability model of an idealized unidirectional reinforcement consisting of regularly ordered, parallel fibers was derived both for flow along and perpendicular to the fibers by Gebart [3]. In the present work we approach the problem similar to Gebart; however, here we consider the partially impregnated layers of prepregs, the so called EvaC pregpregs [4]. In such a prepreg the fiber bed is kept dry and the matrix cover both sides of the preform, as shown in Figure 2. Therefore, we assume that during the manufacturing processes two kinds of flow will develop; (i) the macroscopic flow

between the layers and (ii) the infiltration flow into the dry fiber bed. In summary, the flow is restricted perpendicular to the plies and fairly unrestricted parallel to the plies.

The goal of this paper is to combine the theory of porous media with respect to the liquid resin infusion problem, as developed in [1], with the constitutive relation for anisotropic permeability introduced in following section.

2 A homogenized theory of porous media

The fiber bed during infusion is considered as a porous material with a fibre bed with pores that are either partially filled by liquid resin or contains unfilled void space. The macroscopic volume fractions for the solid and the fluid phases n^s and n^f, respectively, are defined as

$$n^s = \frac{V^s}{V}, \qquad n^f = \frac{V^f}{V} \qquad \text{with} \qquad n^s + n^f = 1 \tag{2}$$

where V^s is the volume portion of the solid relative to a representative volume with volume V, and V^f is the compressible fluid volume portion of the pore space. The volume fractions are connected via the saturation constraint [1].

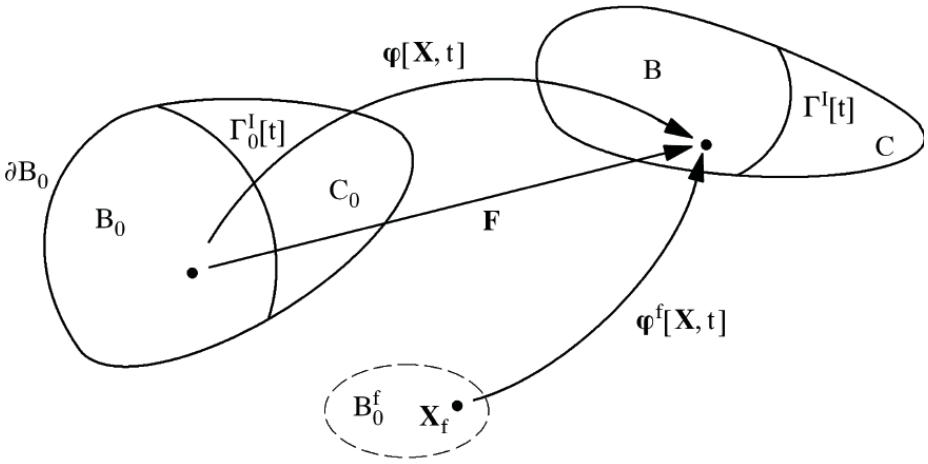

Figure 1. Reference and spatial configurations representing infusion of fiber bed with partially saturated and unsaturated regions B and C, respectively. The free surface $\Gamma_0^l[t]$ is migrating in the material and separates the regions B_0 and C_0.

The fluid phase mixture may be further described upon introducing the degree of liquid saturation $0 \leq \xi[x,t] \leq 1$, where $\xi = 0$ corresponds to gas-filled pores and $\xi = 1$ corresponds to the situation of complete liquid saturation.

1.1 Governing equations

To formulate the coupled problem of partially fluid saturated solid, mass balance and momentum balance is used

$$\rho^f \boldsymbol{\nabla} \cdot \boldsymbol{v} - n^f \dot{\rho}^f = -\boldsymbol{\nabla} \cdot (\rho^f \boldsymbol{v}^d), \tag{3}$$

$$\overline{\boldsymbol{\sigma}} \cdot \nabla + \hat{\rho} \boldsymbol{g} = \mathbf{0} \quad \forall \boldsymbol{x} \in B, \tag{4}$$

where $\boldsymbol{v}^d$ is the Darcian velocity defined as $\boldsymbol{v}^d = n^f \boldsymbol{v}^r$ and $\overline{\boldsymbol{\sigma}} = \boldsymbol{\sigma}^s + \boldsymbol{\sigma}^f$ is the total Cauchy stress. In turn, $\overline{\boldsymbol{\sigma}}$ is related to the effective (constitutive) stress $\boldsymbol{\sigma}$ and the fluid pressure p via the Terzaghi effective stress principle as $\overline{\boldsymbol{\sigma}} = \boldsymbol{\sigma} - p\mathbf{1}$.

3 Constitutive equations

It turns out that the total mechanical dissipation D may be interpreted in terms of a few independent phenomenological mechanisms of the mixture material.

$$D = \underbrace{\boldsymbol{\sigma}:\boldsymbol{l} - \dot{\psi}}_{D^s} + \underbrace{n^f p \frac{\dot{\rho}^f}{\rho^f} - \hat{\rho}^f \dot{\psi}^f}_{D^{nvf}} + \underbrace{\xi^{-1}\boldsymbol{v}^d \cdot (\underbrace{\rho^f \boldsymbol{g} - \boldsymbol{\nabla} p}_{\boldsymbol{h}_e^f})}_{D^i} \geq 0, \tag{5}$$

where the different terms D^s, D^{nvf} and D^i represent dissipation contributions due to solid deformation, fluid compressibility and Darcian interaction. In equation (5), $\boldsymbol{h}_e^f$ is the effective drag force and it may be noted that the effective stress felt by the continuum is represented by the Terzaghi stress $\boldsymbol{\sigma}$, p is the fluid pressure, $\boldsymbol{l}$ is the spatial velocity gradient, $\hat{\boldsymbol{\rho}}^{\boldsymbol{s}}$ is the bulk density, ψ is free energy and **g** is gravity.

Guided by the dissipation inequality, we outline the constitutive relations of our two-phase continuum in respect to effective stress and Compressible liquid-gas response.

3.1 Effective stress response

Assuming hyper-elasticity for the effective stress response for a Neo-Hookean elastic material we obtain the free energy $\psi\,[\boldsymbol{C}]$ for the solid phase which correspond constitutive state equations as

$$\boldsymbol{S} = 2\hat{\rho}_0^s \frac{\partial \psi}{\partial \boldsymbol{C}}, \tag{6}$$

$$p = (\rho^f)^2 \frac{\partial \psi^f}{\partial \epsilon}, \tag{7}$$

where $\boldsymbol{S} = \overline{\boldsymbol{S}} - J\boldsymbol{C}^{-1}p$ is the consequent effective second Piola Kirchhoff stress due to the Terzaghi effective stress principle.

3.2 Compressible liquid-gas response

In order to assess the pressure dependence in the fluid density, it is assumed that the same pressure prevails in the liquid and gas constituents and that the highly compressible gas constituent is pressure dependent in the spirit of the ideal gas law. It should be noted that the rate behavior of the fluid density may be characterized in terms of the compression modulus of the liquid-gas mixture.

$$\rho^f = \xi\rho^l + (1-\xi)\rho^g \tag{8}$$

$$\dot{\rho}^f = \frac{1}{K^f}\dot{p} + (\rho^l - \rho^g)\dot{\xi} \quad with\ K^f = \frac{1}{(1-\xi)k^g} \tag{9}$$

Indeed, the value of K^f increases for increased saturation and decreased gas-compliance k^g. For continued saturation towards $\xi = 1$, we obtain that $K^f \to \infty$ and $\xi = 0$ leading to fluid incompressibility, i.e. $\rho^f \to \rho^l$. c.f. Larsson et. al. [1] for further details.

3.3. Solid-fluid interaction

A key feature of the present contribution is the solid-fluid interaction model, where it is assumed that two types of flow will develop during the composites processing; (i) the macroscopic flow between the layers and (ii) the infiltration flow into the dry fiber bed. In this context, the generic flow in porous media may be described using the Darcy law as

$$\boldsymbol{v}^d = -\frac{1}{\nu(1-\phi^p)}\boldsymbol{K}\cdot\boldsymbol{h}_e^f, \tag{10}$$

where $\boldsymbol{K}$ is the anisotropic permeability tensor and ν is liquid viscosity. To derive the permeability for the considered fibre bed, let us introduce the structural tensor $\mathbf{M} = \mathbf{T} \otimes \mathbf{T} \in \mathrm{B}_0$, where **T** is a unit vector transverse to the fibre bed as shown in Figure 2.

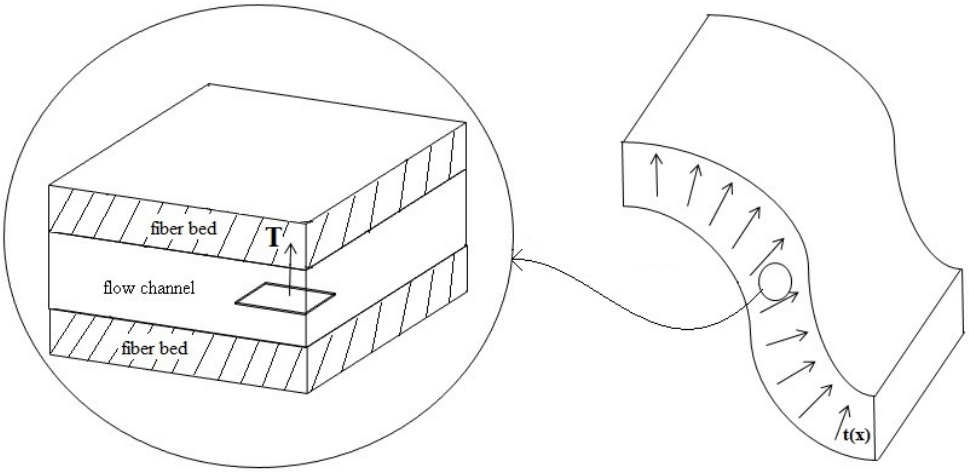

Figure 2. Flow channel and fiber bed stacks

Projecting the total Darcian flow on to the director field **T** and the plane perpendicular to **T** gives

$$\boldsymbol{v}^d = -\frac{1}{\nu(1-\phi^p)}\left(K_t(\mathbf{1}-\boldsymbol{M}) + K_{fB}\boldsymbol{M}\right)\cdot\boldsymbol{h}_e^f, \tag{11}$$

where $K_{\boldsymbol{fB}}$ is the permeability in the **T**-direction and K_t is the permeability perpendicular to **T**. Following the development in [5], the permeability K_t may be represented as the linear mixture rule $K_t = K_{fB}(1-\phi_l) + K_{Ch}\phi_l$, leading to

$$\boldsymbol{v}^d = -\frac{1}{\nu(1-\phi^p)}\left(\left(K_{fB}(1-\phi_l) + K_{Ch}\phi_l\right)(\mathbf{1}-\boldsymbol{M}) + K_{fB}\boldsymbol{M}\right)\cdot\boldsymbol{h}_e^f, \tag{12}$$

where K_{fB} is the permeability through the fiber, K_{Ch} is the permeability through the channel and ϕ_l is liquid volume fraction.

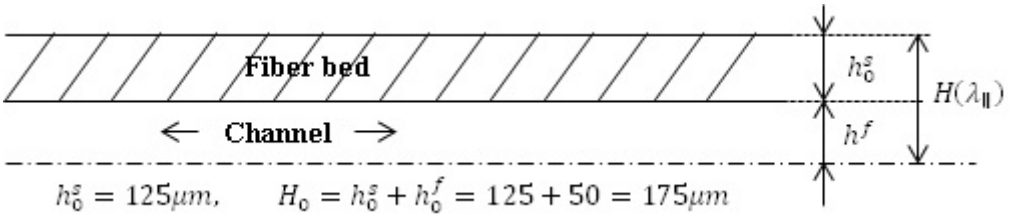

Figure 3. Distance between fiber layers and flow channel

The permeability through the fiber bed K_{fB} is represented using the Gebart equation as in (12). The permeability through the channel may be approximated considering the resistance to viscous flow within a rectangular channel, [5]

$$K_{fB} = \frac{16r^2}{9\pi\sqrt{2}}\left[\sqrt{\frac{\pi}{2\left(\frac{\phi_0}{J}\right)\sqrt{3}}} - 1\right]^{\frac{5}{2}}, \tag{13}$$

$$K_{Ch} = \frac{(h^f)^2}{12}, \tag{14}$$

where h^f is the channel height and it is a function of the continuum stretch parallel to **T** defined as

$$h^f = H(\lambda_\parallel) - h_0^s \rightarrow \{H(\lambda_\parallel) = H_0\lambda_\parallel\} \rightarrow h^f = H_0\lambda_\parallel - h_0^s, \tag{15}$$

where $\lambda_\parallel$ is the stretch in the direction of **T** given as

$$\lambda_\parallel = \sqrt{\boldsymbol{C}:\boldsymbol{M}}, \tag{16}$$

and $\boldsymbol{C}$ is the right Cauchy-Green deformation tensor, h_0^s is the fiber ply thickness (assumed constant at the moment) and $H_0 = h_0^s + h_0^f$. In consequence, the channel permeability reads

$$K_{Ch} = \frac{(H_0\lambda_\parallel - h_0^s)^2}{12}. \tag{17}$$

When the preform deforms, the size of the channel decreases, meaning that ϕ_l & $h^f \rightarrow 0$, which in that case K_{Ch} vanishes.

3.4 A smooth free surface problem

In order to formulate the governing equations of the two different continua, one may generally distinguish one fluid saturated portion $B_0 \rightarrow B_0[t]$ and one non-saturated one-phase portion $C_0 \rightarrow C_0[t]$ separated by the free surface boundary $\Gamma^I[t]$, as shown in Figure 1. However, the key idea of paper is to consider the motion $\Gamma^I[t]$ in terms of the evolution of the fluid saturation field $\xi = \xi[\boldsymbol{x}, t]$. Clearly, at the initiation of a wetting process the initial condition is that $\xi[\boldsymbol{x}, t] = 0$ in order to define the one phase non-wet region, whereas the fully saturated region is defined by $\xi[\boldsymbol{x}, t] = 1$. We thereby replace the strictly discontinuous free surface problem by a smooth transition of the liquid front in terms of the evolution of the fluid

saturation field $\dot{\xi} = \dot{\xi}[\boldsymbol{x}, t]$. We can recall the saturation evolution [1] along with the Darcian flow model which is to be satisfied locally according to

$$n^f \dot{\xi} + \frac{\dot{J}}{J}\xi + \boldsymbol{\nabla} \cdot \boldsymbol{v}^d = 0 \tag{18}$$

whereby the saturation degree variable may be regarded as a local field variable $\xi = \xi[\boldsymbol{x}, t]$ or, simply, as an internal variable governed by equation (18).

4 Total solution procedures

The planar infusion problem shown in Figure 4 is considered for numerical simulation. The applied pressure load due to the vacuum infusion is prescribed along all the external boundaries, except at the impermeable lower boundary in Figure 4. The solid deformation is also controlled via prescribed displacement along the lower, impermeable boundary in the figure. The wetting process is driven by the Darcian solid-fluid interaction force as induced by pressure gradient. This process is manifested by a migrating resin flow front represented by the saturation degree evolution with time in the porous fiber bed.

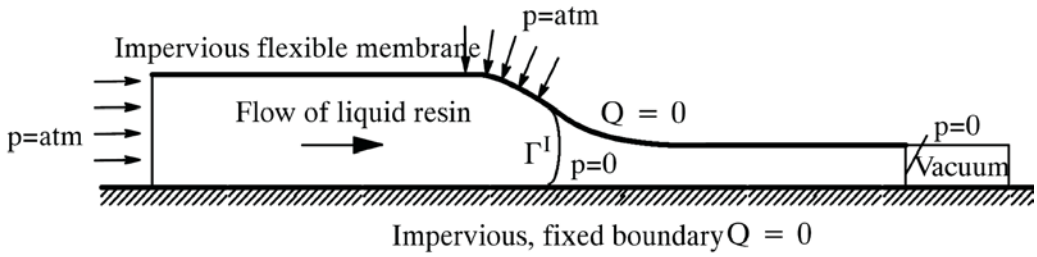

Figure 4. Liquid resin infusion of fiber bed principle for specimen subjected to vacuum induced pressure load

The material parameters used in the numerical simulation are the same as what has been used in [1].

5 Numerical results and concluding remarks

A simulation of liquid resin infusion, as defined in Figure 4, with a flexible fiber bed based on hyper elastic material model is considered using the same boundary conditions and material parameter as in Larsson et. al. [1]. The goal is to assess the permeability model developed in this paper invoked to the infusion simulation algorithm.

As to the assessment of the global saturation degree for the numerical solution, we simply consider ξ as the average value of the saturation degree in the elements, i.e. $\overline{\xi} = < \xi >$.

In Figure 5, the deformation of the preform is shown along with the distribution of ξ. A non-uniform compaction of the preform is induced by the vacuum pressure and so is the temporal evolution of the diffusive flow front. During the infusion, as the fluid pressure increases, some of the deformation will be balanced off, leading to a difference in deformation in the saturated and in the non-saturated regions. Preform deformation has a direct influence on the permeability, porosity and the Darcian liquid flow advancement. Figure 6 shows the resulting fluid pressure distribution, which is the key mechanism driving the resin infusion via the anisotropic permeability. As time passes, the Darcian velocity decreases due to the decrease in the pressure gradient, and the process is significantly slowed down, as shown in Figure 7. The convergence of the solution upon mesh refinements is also shown in Figure 7 and it can be noted that the total infusion time is around $T \approx 60$ minutes.

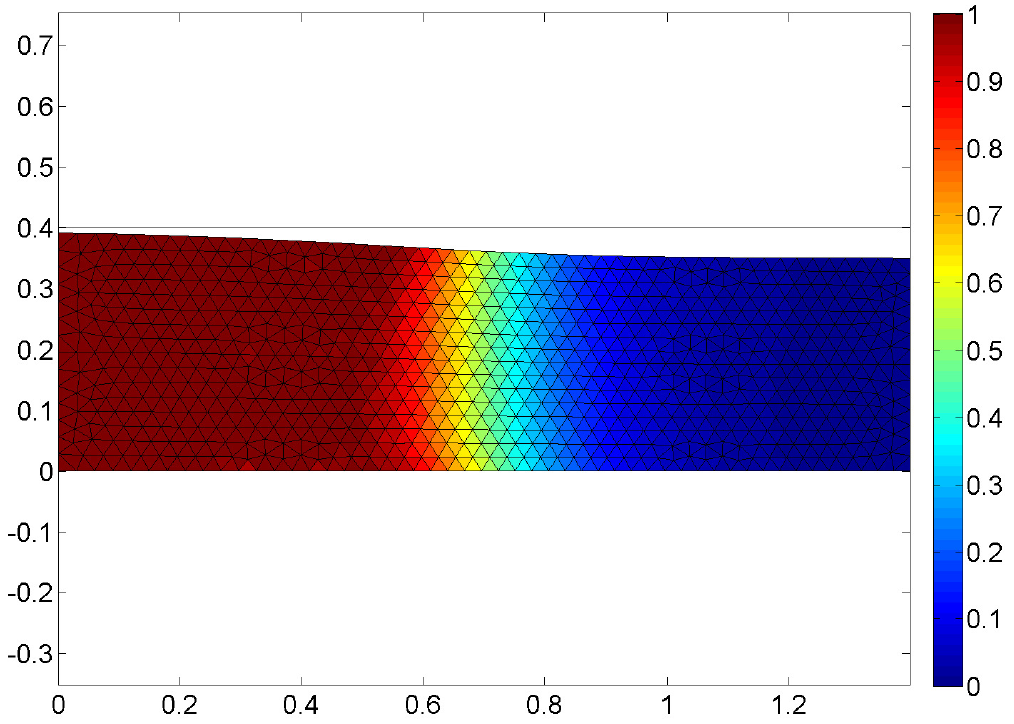

Figure 5. Preform deformation during infusion process along with current state of saturation

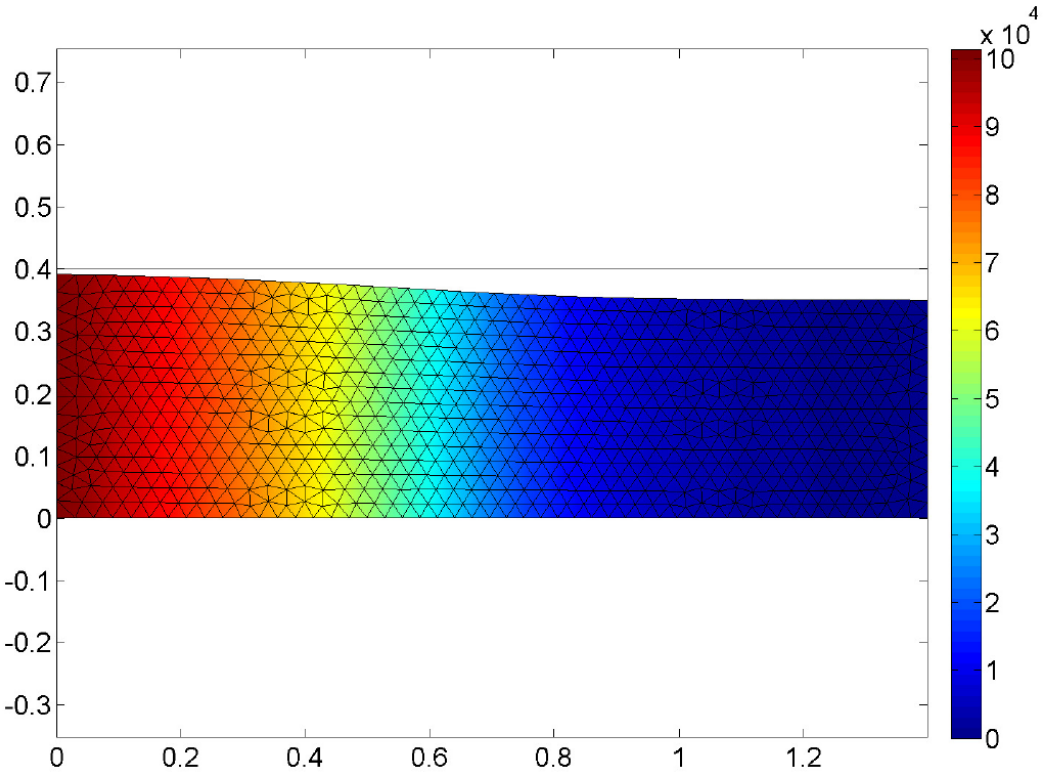

Figure 6. Preform deformation during infusion process along with fluid pressure distribution

In the present paper we have framed the liquid resin infusion of composites (and other related processes) into a free surface formulation based on two-phase porous media theory while the driving flow is modeled by Darcy law with an anisotropic permeability model. As compared to other methods available in the literature for these types of problems, typically restricted to simplified 1D approximations with isotropic assumption for the flow, the approach is quite general in the sense that it provides the coupling between the preform deformation and the free surface migration in one and the same formulation considering flow properties different in different directions.

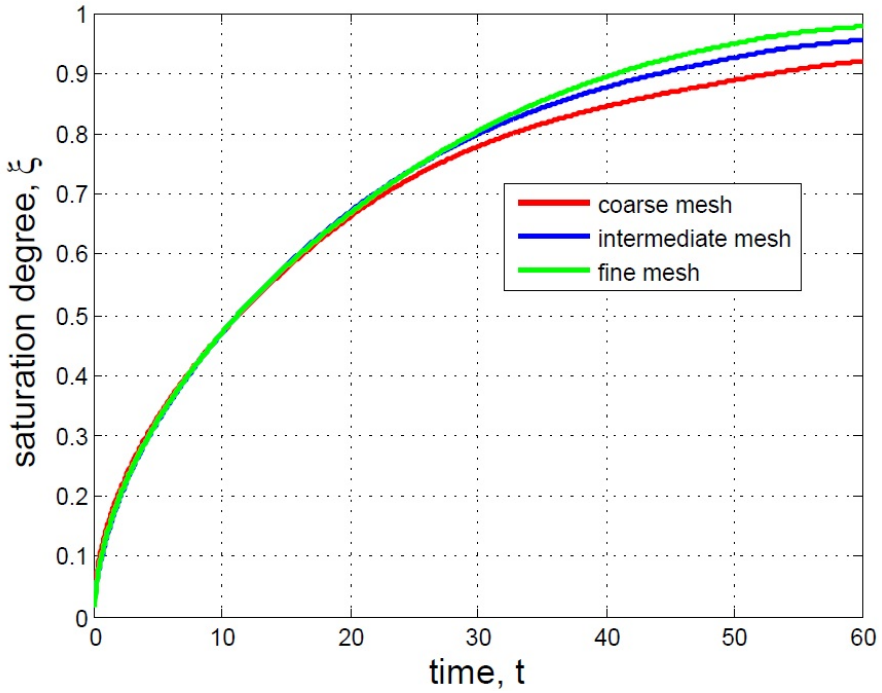

Figure 7. *Global saturation degree versus time, mesh sensitivity analysis*

5 References

[1] Larsson, R., Rouhi, M., Wysocki, M., "Free surface flow and preform deformation in composites manufacturing based on porous media theory", European Journal of Mechanics A/Solids 31 (2012) 1-12

[2] Carman, P. C. 1937, Fluid flow through granular Bed, Transaction institution of chemical engineering, 15:150-166.

[3] Gebart, B. R., Permeability of unidirectional reinforcement for RTM, Journal of composite materials, v 26, No. 8/1992, p1100-1133

[4] Thomas, S., Bongiovanni, C., Nutt, S.R., In situ estimation of through-thickness resin flow using ultrasound, 2008, Composites Science and Technology 68 (15-16), pp. 3093-3098

[5] Dynamics of Fluids in Porous Media, Jacob Bear, Dover Civil and Mechancial Engineering, 1988